Resonant holography

Arnab Sinha and George Barbastathis

Department of Mechanical Engineering, Microsystems Technology Laboratories, and Micro-Photonics Center, Massachusetts Institute of Technology, Cambridge, Massachusetts 02139-4307

Received September 27, 2001

We present a method of enhancing the diffraction efficiency of a hologram by placing it inside a resonant optical cavity. The diffraction efficiency improves on account of the multiple passes that the incident light undergoes inside the optical cavity. The resonance condition in this case turns out to involve both mirror reflectivity and the optical path length inside the cavity. Experimental results for a resonantly enhanced angle-multiplexed holographic memory and an optical three-port element are shown.

OCIS codes: 090.0090, 210.2860, 050.1940, 260.5740.

Volume holographic optical elements have been used in optical interconnects,[1] data storage,[2,3] and imaging.[4] For most applications, the hologram should diffract the highest amount of incident light possible; the undiffracted light is wasted. Here we show that diffraction efficiencies approaching 100% are obtained when the hologram is placed inside an optical cavity and demonstrate the idea experimentally in the context of two applications: an angle-multiplexed holographic memory with increased dynamic range and an optical three-port element.

Re-entrant diffraction into ring resonators has been used in the past for image storage and associative recall,[5,6] and diffraction into Fabry–Perot-type optical cavities has been used for optical interconnects.[7,8] Instead, we tune the cavity to resonate the diffracted beam by multiple passes of the readout beam through the hologram.

Resonant holograms are recorded conventionally by interfering mutually coherent reference and object beams inside a photosensitive medium.[9] After recording is complete, the hologram is placed inside an optical cavity and probed with a beam that replicates as closely as possible the reference beam used during the recording phase. For brevity, we limit the present discussion to the Bragg diffraction regime. However, our results may also be extended to the Raman–Nath regime if multiple diffracted orders are taken into account.

In the resonator shown in Fig. 1(a) with normal incidence of the readout beam, both the forward- and backward-propagating on-axis probe beams are Bragg matched. Therefore, a forward reconstruction and a phase-conjugate reconstruction are obtained simultaneously. Resonance is obtained when all diffracted beams interfere constructively. Optical losses (absorption, scatter) place an upper limit on the resonant diffraction efficiency. The finesse of the holographic cavity is defined by the losses in combination with the single-pass efficiency of the hologram.

Let r denote the amplitude reflection coefficient of the partially reflecting mirror and η_1 the single-pass diffraction efficiency of the hologram (which is obtained from the stand-alone hologram, without the optical cavity). Also, let λ denote the wavelength, b the one-pass intensity loss coefficient inside the cavity, and L the optical path length of the cavity. In terms of these parameters, the forward and the phase-conjugate diffraction efficiencies obtained from the hologram inside the cavity are, respectively,

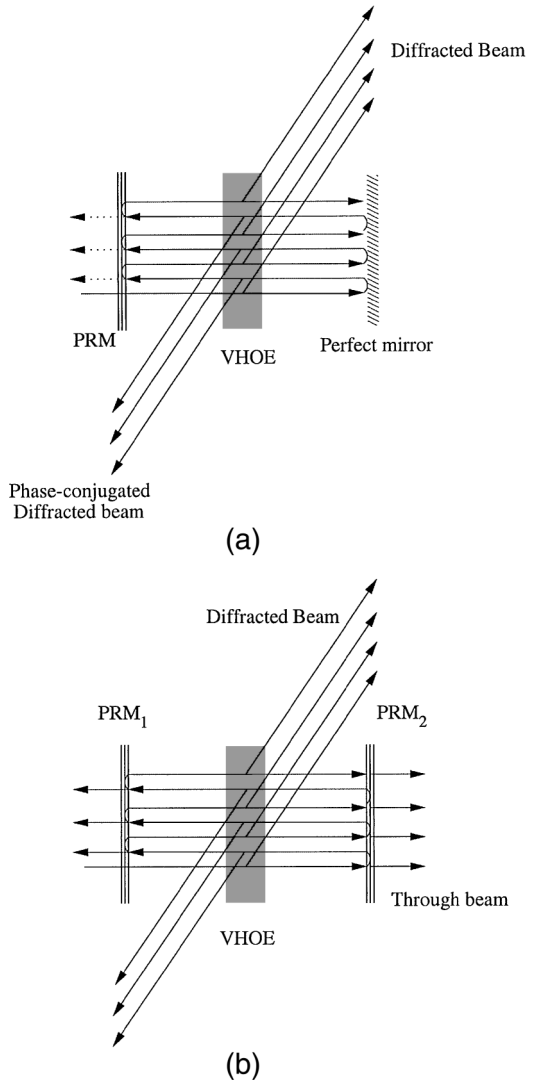

Fig. 1. Geometries for resonant holography: (a) two-port geometry with normal incidence, (b) three-port geometry with normal incidence. VHOEs, volume holographic optical elements; PRMs, partially reflecting mirrors.

0146-9592/02/060385-03$15.00/0

$$\eta_{\mathrm{fw}} = \frac{\eta_1(1-r^2)}{1+r^2(1-\eta_1-b)^2+2r(1-\eta_1-b)\cos(4\pi L/\lambda)}, \tag{1}$$

$$\eta_{\mathrm{pc}} = \eta_{\mathrm{fw}}(1-\eta_1-b). \tag{2}$$

By requiring that no optical power be reflected backward in the direction of the source, we obtain the resonance conditions

$$r = 1-\eta_1-b, \tag{3}$$

$$L = (2m+1)\frac{\lambda}{4}, \tag{4}$$

where m is an arbitrary integer. The quality factor of the holographic resonator is approximately $Q = 1/(b+\eta_1)^{1/2}$. Therefore, the coherence length of the incident beam should be larger than QL to ensure that Eq. (4) can be observed. When these conditions are satisfied, the resulting overall (forward plus phase-conjugate) resonant diffraction efficiency is

$$\eta_\infty = \frac{\eta_1}{\eta_1+b}. \tag{5}$$

Since $\eta_1 + b < 1$, the resonant gain $G = \eta_\infty/\eta_1$ is always larger than 1. However, the single-pass loss coefficient b sets an upper limit on the attainable resonant gain. Resonance is most efficient when $\eta_1 \gg b$. Alternatively, losses may be compensated for by inclusion of optical gain inside the holographic cavity.

Resonance conditions (3) and (4) apply to arbitrary diffracted wave fronts. Spatial frequency components having equal diffraction efficiencies resonate simultaneously if they satisfy condition (3). This is verified in the experiment illustrated in Fig. 2. However, spatial frequency components whose diffraction efficiencies deviate from condition (3) get filtered out because they are nonresonant. The sensitivity of the holographic resonator to η_1 is shown in Fig. 3. These curves indicate that reconstructions degrade gracefully as a result of recording nonuniformities. However, resonance is extremely sensitive to path-length condition (4) as in any Fabry–Perot-type cavity.[10] As in other resonant configurations, the path sensitivity of resonant holograms has potential applications to interferometric sensing[11,12] and wavelength routing.[13]

We implemented a simple resonant holographic memory by mounting the holographic material of Fig. 1(a) on a rotation stage. We superimposed plane-wave holograms at several angular positions, separated by twice the Bragg selectivity of the material. Figure 4 shows the resonant diffraction efficiency enhancement that we obtained by Bragg matching and resonating each hologram individually. Resonance resulted in improvement of the average M number[14] by a factor of $\sqrt{G} \approx 3.4$ in our experiment.

Two methods can be used to eliminate the phase-conjugate reconstruction: oblique incidence of the readout beam to the Fabry–Perot cavity and a ring resonator.[15] The former presents problems in practice because the resonant beam walks off the resonator in the lateral direction.

The geometry of Fig. 1(b) is similar to that of Fig. 1(a), except that the back mirror has been replaced with a partially reflecting mirror with amplitude reflection coefficient r'. Thus, this device acts as an optical three-port element. The amplitude resonance condition is

$$r = r'(1-\eta_1-b), \tag{6}$$

and the overall (forward plus phase-conjugate) resonant diffraction efficiency is

$$\eta_\infty = \frac{\eta_1(1+rr')}{1-r^2}. \tag{7}$$

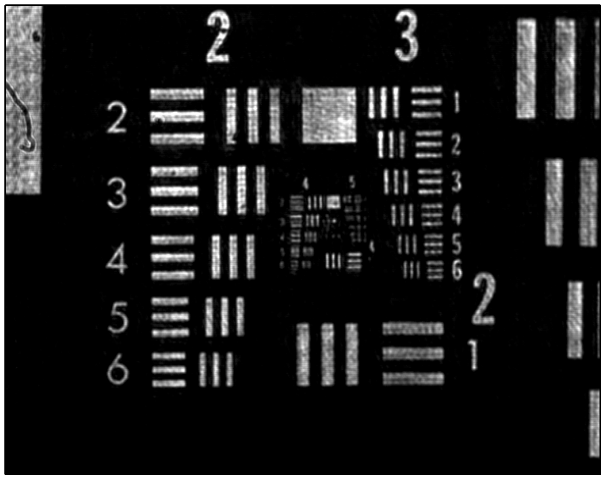

(a)

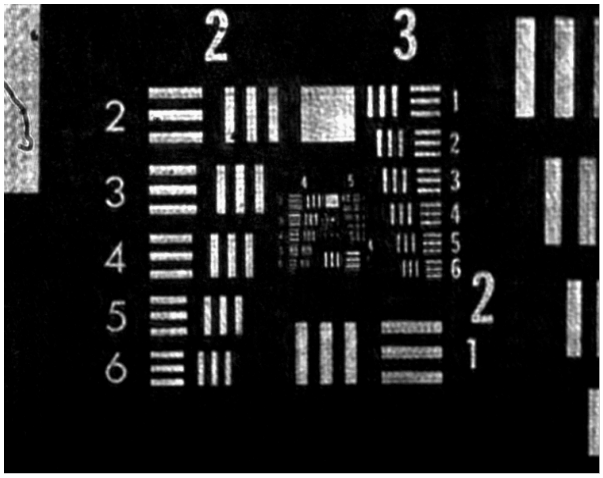

(b)

Fig. 2. Holographic reconstruction: (a) nonresonant, (b) resonant. We recorded a hologram of a U.S. Air Force Resolution Chart slightly off the Fourier plane to ensure equal diffraction efficiencies for a wide bandwidth of plane-wave components. The resonant reconstruction was obtained with the configuration shown in Fig. 1(a) with $r^2 = 0.9$. The measured loss coefficient was $b = 0.07$, and the diffraction efficiencies were $\eta_1 = 0.3\%$ and $\eta_{\mathrm{fw}} = 1.5\%$ (theoretical, 2.0%). This and subsequent experiments were implemented on a 1-mm-thick slab of Fe-doped $LiNbO_3$ with a doubled Nd:YAG laser ($\lambda = 532$ nm).

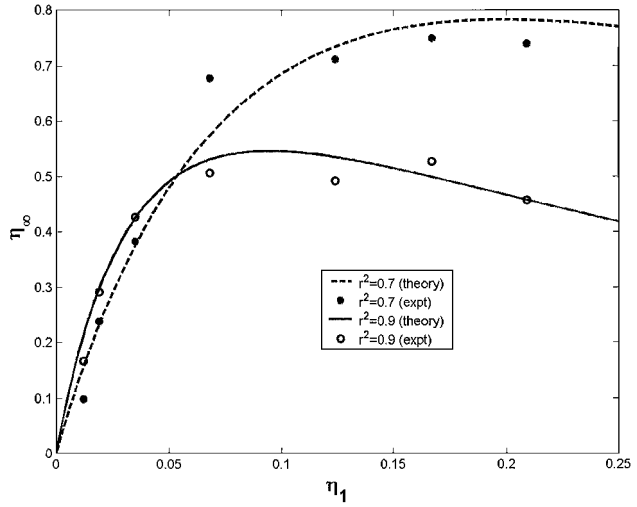

Fig. 3. Theoretical and experimental diffraction efficiencies ($\eta_{\mathrm{fw}} + \eta_{\mathrm{pc}}$) from Eqs. (1) and (2) that satisfy Eq. (4) versus one-pass efficiency, η_1, for two partially reflecting mirror reflectivities. A measured loss coefficient of $b = 0.05$ was used for the theoretical curves. The experimental curves were obtained with a lateral aperture of $\approx 1\ \mathrm{mm}^2$, where resonance was relatively uniform.

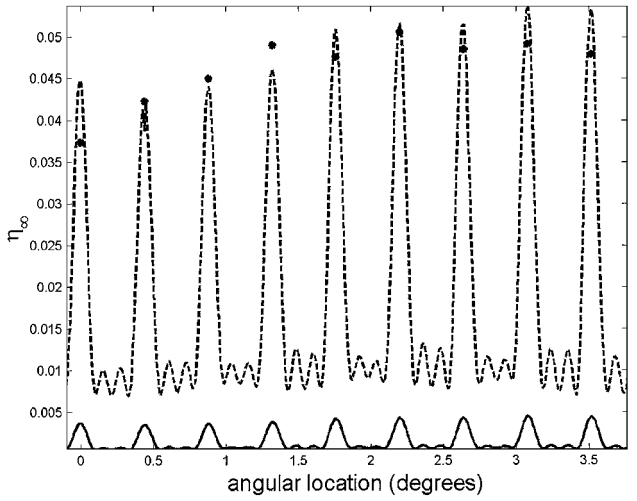

Fig. 4. Holographic memory with resonant enhancement of the diffraction efficiency. The solid curve was obtained by angular scanning of the memory without the resonator. Each peak corresponds to one stored hologram. The dashed curve was obtained by application of Eqs. (1), (2), and (4) to the experimental data of the solid curve. The asterisks are actual values of the corresponding resonant diffraction efficiencies obtained experimentally.

The fraction of the power transmitted straight through the hologram and the two partially reflecting mirrors is

$$\eta_{\mathrm{trans}} = \frac{r(1 - r'^2)}{r'(1 - r^2)}. \tag{8}$$

The sensitivity of this element to deviation of η_1 from resonance condition (6) is shown in Fig. 5. One can think of the resonant three-port element as an efficienct, smart beam splitter, defining both the amplitude and the phase of the deflected beam relative to the readout beam.

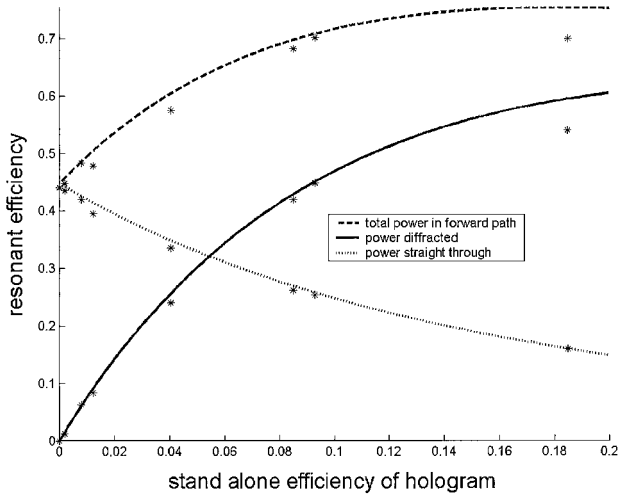

Fig. 5. Experimental and theoretical responses of the three-port element of Fig. 1(c) with $r^2 = 0.7$, $r'^2 = 0.9$, and $b = 0.05$.

In conclusion, resonant holograms are compatible with and improve the diffraction efficiency of many holographic systems. We have obtained preliminary evidence that resonant holograms are also superior in terms of other performance metrics, e.g., depth resolution in ranging systems.

This research was supported by the U.S. Air Force Research Laboratories (Munitions Division AFRL/MNG, Eglin Air Force Base). We are grateful to D. Psaltis and H. I. Smith for helpful discussions and to one anonymous reviewer for constructive criticism. The authors' e-mail addresses are arnab@mit.edu and gbarb@mit.edu.

References

1. D. Psaltis, D. Brady, X. G. Gu, and S. Lin, Nature **343,** 325 (1990).
2. J. F. Heanue, M. C. Bashaw, and L. Hesselink, Science **265,** 749 (1994).
3. D. Psaltis and F. Mok, Sci. Am. **273,** 70 (1995).
4. G. Barbastathis and D. J. Brady, Proc. IEEE **87,** 2098 (1999).
5. D. Psaltis and N. Farhat, Opt. Lett. **10,** 98 (1985).
6. D. Z. Anderson, Opt. Lett. **11,** 56 (1986).
7. W. H. Steier, G. T. Kavounas, R. T. Sahara, and J. Kumar, Appl. Opt. **27,** 1603 (1988).
8. S. A. Collins and H. J. Caulfield, J. Opt. Soc. Am. A **6,** 1568 (1989).
9. D. Gabor, Nature **161,** 777 (1948).
10. A. Yariv, *Optical Electronics*, 4th ed. (Saunders, Philadelphia, Pa., 1991).
11. D. Z. Anderson, Opt. Lett. **9,** 417 (1984).
12. A. Bearden, M. P. O'Neill, L. C. Osborne, and T. L. Wong, Opt. Lett. **18,** 238 (1993).
13. M. A. Scobey, W. J. Lekki, and T. W. Geyer, Laser Focus World **33**(3), 111 (1997).
14. F. Mok, G. W. Burr, and D. Psaltis, Opt. Lett. **21,** 896 (1996).
15. The possibility of using a ring resonator was pointed out to us by D. A. B. Miller.